

# Assessment of atherosclerosis in large vessel walls: A comprehensive review of FDG-PET/CT image acquisition protocols and methods for uptake quantification

Saeid Gholami, MD,<sup>a</sup> Ali Salavati, MD, MPH,<sup>a</sup> Sina Houshmand, MD,<sup>a</sup> Thomas J. Werner, MSE,<sup>a</sup> and Abass Alavi, MD, MD (Hon), PhD (Hon), DSc (Hon)<sup>a</sup>

<sup>a</sup> Department of Radiology, Hospital of the University of Pennsylvania, Philadelphia, PA

Received Oct 22, 2014; accepted Jan 5, 2015  
doi:10.1007/s12350-015-0069-8

**There is growing evidence showing the importance of fluorodeoxyglucose positron emission tomography (FDG-PET) in the evaluation of vessel wall inflammation and atherosclerosis. Although this imaging modality has been increasingly used, there are various methods for image acquisition and evaluating FDG uptake activity in the vessel walls and atherosclerotic lesions, including qualitative visual scaling, semi-quantitative, and quantitative evaluations. Using each of these image acquisition protocols and measurement methods may result in different findings. In this review, we are going to describe the various image acquisition methods and common measurement strategies reflected in the literature and discuss their advantages and flaws.**

**Key Words: Atherosclerosis • fluorodeoxyglucose • positron emission tomography • measurement • quantification**

---

**See related editorial, pp. 480–482**

---

## INTRODUCTION

Fluorine-18-fluorodeoxyglucose positron emission tomography/computerized tomography (FDG-PET/CT) is an imaging modality that has been utilized for evaluating atherosclerosis and vascular inflammation non-invasively.<sup>1,2</sup> Vascular findings using this modality have been associated with traditional CVD risk factors,<sup>3,4</sup> Framingham risk scores,<sup>5</sup> and molecular markers such as vascular cell

adhesion molecule-1, CD-68, and C-reactive protein.<sup>2,5,6</sup> This imaging technique is capable of detecting vessel atherosclerosis lesions;<sup>7</sup> monitoring plaque progression<sup>8,9</sup> and vulnerability<sup>10</sup>; and visualizing the effects of interventions on vessel wall inflammation and atherosclerosis.<sup>11-14</sup> Despite widespread usage of this scanning modality, a variety of methodologies have been used for pre-scan patient preparation, image acquisition, and measurement of FDG uptake activity in vessel wall.<sup>3,14-17</sup> These methodologies may lead to different image qualities and inconsistent final findings.<sup>18-20</sup> Herein, we show the different patient preparation and image acquisition protocols and describe their influences on image quality and final findings. Also, we summarize common measurement indices and quantification methods and discuss their strengths and weaknesses.

## PATIENT PREPARATION AND BLOOD GLUCOSE LEVEL

Protocols for preparing subjects for FDG-PET/CT imaging of large vessel walls (other than the coronary

Reprint requests: Saeid Gholami, MD, Department of Radiology, Hospital of the University of Pennsylvania, 3400 Spruce St, Philadelphia, PA 19104; [saeid.gholami@uphs.upenn.edu](mailto:saeid.gholami@uphs.upenn.edu)

J Nucl Cardiol 2015;22:468–79.

1071-3581/\$34.00

Copyright © 2015 American Society of Nuclear Cardiology.

arteries) have been mostly based on a period of fasting between 4 and 12 hours<sup>21</sup> regardless of the target vessel or the other characteristics of the subjects. To our knowledge, the effect of pre-scan diet instructions on the FDG uptake measurements of the large vessels has not been well studied.

For patients who follow the appropriate diet, investigators expect blood glucose concentration lower than a specific level. This level varies from 126 to 200 mg·dl<sup>-1</sup><sup>15,22,23</sup> in different studies. Bucierius et al showed that higher blood glucose level mostly decreases vessel wall but increases venous blood pool FDG level measurement.<sup>20</sup> It has been suggested that reproducibility of vessel wall FDG uptake measurements is worse in subjects with blood glucose level higher than normal (126 mg·dl<sup>-1</sup>). Therefore, blood glucose level less than 126 mg·dl<sup>-1</sup> is preferred for these type of studies.<sup>20</sup>

### FDG INJECTION DOSE

The dose of FDG differs among research groups and has been administered as low as 185 to 481–925 MBq.<sup>24–26</sup> Increasing FDG dose does not necessarily improve the FDG uptake measurements and final results.<sup>20</sup> A dose between 307 and 458 MBq has been suggested as appropriate dose for vessel assessments.<sup>20</sup> Moreover, as reported by Davies et al, a low dose of 185 MBq will still give adequate image quality and sufficient information about vessel walls inflammatory activity.<sup>24</sup>

### INJECTION-TO-SCAN TIME INTERVAL, EARLY VS DELAYED IMAGING

The applied time interval between FDG injection and PET image acquisition has been from 30 to 45 minutes<sup>27</sup> to around 210 minutes<sup>28</sup> among studies. Early time points are practical for center feasibility and patient comfort<sup>29</sup> but improved target-to-background contrast is typically achieved by delayed imaging.<sup>19,20</sup> Some studies suggest that circulation time longer than 1.5 hour improves visualization of vessel wall atherosclerosis because vessel walls and lesions are more distinguishable as background activity decreases.<sup>19,20,30,31</sup> However, this has not always been confirmed.<sup>29,32</sup>

Regarding pathological and clinical characteristics, FDG uptake measured by single-time point studies has had correlation with macrophage numbers,<sup>25,27,33</sup> CVD risk factors,<sup>5,34–36</sup> and clinical events<sup>37,38</sup> at either early or late scans. In a dual-time point imaging study, the association of vessels FDG uptake to CVD risk score was not significantly different between 90 and 180 minutes.<sup>19</sup> Performing more studies about the relation between imaging time point with lesion uptake and clinical and pathological findings may be informative.

### VESSEL WALL FDG UPTAKE MEASUREMENT

Assessment of vascular wall inflammation and atherosclerotic plaque FDG uptake activity was initiated by qualitative and visual scaling methods<sup>3,35</sup> and changed over time to semi-quantitative and quantitative methods.<sup>14–17</sup> In the recent years, most studies prefer to use semi-quantitative and quantitative measurements to evaluate FDG uptake activity of the vessel walls and atherosclerosis.<sup>4,39–41</sup> To measure the vessel wall FDG uptake in a PET/CT image, regions of interest are placed around the outer boundaries of vessel walls in trans-axial views of PET/CT scan (either with or without contrast) (Figure 1A). Table 1 has summarized some semi-quantitative measurement indices that have been used by investigators. After measuring these semi-quantitative indices, some groups have described their own strategy for improving evaluation of FDG uptake activity in the plaques and inflammatory lesions within vessel walls and for comparing the disease activity between and within subjects precisely. These additional measurement strategies include index vessel selection and most diseased segment and active segment analysis,<sup>42</sup> atherosclerosis burden and global inflammatory burden,<sup>43</sup> global metabolic activity,<sup>44</sup> and coverage extension and skipping the slices.<sup>45</sup>

### Semi-quantitative Indices

**Standardized uptake value (SUV).** SUV is a factor calculated by dividing decay corrected tissue concentration of FDG at a time point ( $t$ ) by decay corrected total injected FDG at the same time point ( $t$ ) per body weight.<sup>49</sup> Investigators report this index as vessel wall SUVmean<sup>5,8</sup> and/or SUVmax.<sup>8,21,36,50,51</sup> Superiority of each one of SUVmean or SUVmax over the other one is controversial among studies; some studies have reported SUVmean to show wall inflammation with or without atherosclerosis and also to differentiate groups with different CVD risk factors,<sup>16,52</sup> while some other studies have suggested SUVmax as useful index for studying vessel walls.<sup>21,27,36</sup> Other studies report both SUVmax and SUVmean would give similar results.<sup>50</sup> In technical aspects, SUVmax may be preferable because it is less affected by background and blood pool activity<sup>45</sup> but there is increased risk of noise-related bias and loss of precision with SUVmax.<sup>53</sup>

Although it is widely used, SUV has some potential flaws when used as a measurement of FDG uptake in the vessel walls, which may affect the final results. One possible problem with SUV is the partial volume effect where background activity (mainly blood pool) spills over into the region of interest drawn around the vessel wall and atherosclerosis.<sup>19</sup> To resolve this problem, it has been suggested that the blood pool SUV should be

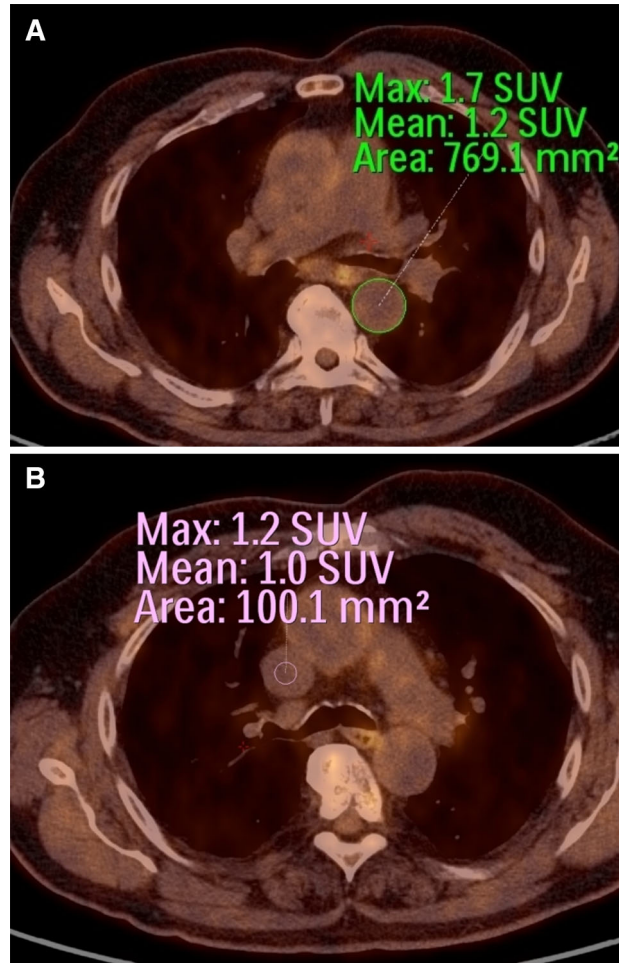


**Figure 1.** Trans-axial views are commonly used to evaluate FDG uptake in the vessel wall. A circular region of interest is placed around the outer boundaries of the vessel (descending aorta) to measure FDG uptake in the vessel wall (A). Then, these numbers should be normalized to background activity which is measured from blood pool by drawing a region of interest inside the vessel (superior vena cava) lumen where there is minimal wall FDG uptake activity (B).

subtracted from the vessel wall and plaque SUV to have wall-to-blood SUV gradient (namely corrected SUV). Corrected SUV may better show the FDG uptake and inflammation in the vessel walls and plaques<sup>1</sup> and is more correlated with CVD risk factors.<sup>19</sup>

Another inaccuracy associated with SUV is that this index is a function of FDG accumulation in 3 parts of a lesion: intracellular fluid, interstitial fluid, and intravascular blood.<sup>53</sup> Therefore, SUV may be affected by neoangiogenesis<sup>54,55</sup> which may develop in atherosclerosis. Clearance rate and blood level of the FDG in each subject can be a potential confounding factor of SUV measurement and comparison.<sup>53</sup> Therefore, it would be helpful to normalize vessel wall SUV with a reference tissue SUV in the same subject.<sup>53</sup>

*Normalization of the background activity.* For normalizing FDG uptake in the vessel walls, various

sites have been used as reference tissue. These sites include the lung<sup>38</sup> as well as blood pool activity which has been measured by placing regions of interest within the lumen of suprarenal descending aorta,<sup>22</sup> aneurysmal abdominal aorta,<sup>56</sup> left atrium,<sup>57</sup> subclavian or internal jugular vein,<sup>23</sup> and most commonly superior and inferior vena cava<sup>58</sup> (Figure 1B). Large veins such as the vena cava and jugular are highly suggested as background because there is higher risk of partial volume effect in the aorta and atria due to great FDG accumulation in the muscular walls and also their motions.

As commonly used in cancer patients, there is possibility of using sites other than blood pool (such as liver or muscle) to normalize vessel measurements for background activities. But it is very important to notice that atherosclerosis is a systemic disease. It has been shown that FDG activity in the spleen<sup>21</sup> and bone

**Table 1.** Simple semi-quantitative measurements used by investigators

| Study                        | Measurement index   |
|------------------------------|---|
| Kim et al <sup>21</sup>      | $\text{SUV} = \frac{\text{decay corrected tissue radioactivity concentration (MBq}\cdot\text{ml}^{-1})}{\text{decay corrected injected activity (MBq)/body weight (kg)}}$   |
| Nirra et al <sup>46</sup>    | $\text{TBR} = \frac{\text{Target Tissue (vessel wall) SUV}}{\text{Background (blood pool) SUV}}$  |
| Rudd et al <sup>33</sup>     | $\text{FDG accumulation rate (sec}^{-1}) = \frac{\text{mean decay-corrected plaque volume of interest FDG concentration (kBq}\cdot\text{mL}^{-1})}{\text{integral of the decay-corrected plasma FDG level (kBq}\cdot\text{mL}^{-1})}$ |
| Ogawa et al <sup>47</sup>    | $\text{Differential uptake ratio} = \frac{\text{tissue activity (kBq)/tissue weight (g)}}{\text{injected radiotracer activity (kBq)/body weight (g)}}$  |
| Ogawa et al <sup>47</sup>    | $\text{Tissue-to-blood radioactivity} = \frac{\text{vessel wall concentration of FDG (kBq}\cdot\text{mL}^{-1})}{\text{blood concentration of FDG (kBq}\cdot\text{mL}^{-1})}$  |
| Ishino et al <sup>48</sup>   | $\text{PET value (non-attenuation corrected images)} = \frac{\text{highest uptake value in the region of interest}}{\text{injected dose}}$  |
| Paulmier et al <sup>38</sup> | $\text{Tissue to background ratio (non-attenuation corrected images)} = \frac{\text{Mean of each maximal arterial wall uptake value per pixel}}{\text{mean lung uptake value per pixel}}$   |

SUV, Standardized uptake ratio; MBq, mega Becquerel; Kg, kilogram; TBR, target-to-background ratio; g, gram

marrow<sup>21</sup> increases in these patients. Moreover, there is an association between vessels inflammatory activity with FDG uptake in visceral fat,<sup>59</sup> subcutaneous<sup>59,60</sup> and pericardial fat,<sup>60</sup> periodontal tissues,<sup>61</sup> and synovia.<sup>62</sup> Therefore, using other tissues than blood pool for normalizing the background activity may affect the final measurements as they may be involved in the systemic inflammatory process of atherosclerosis.

**Target-to-background ratio (TBR).** TBR is calculated by normalizing vessel walls SUV with a reference tissue.<sup>53</sup> TBR seems to represent FDG uptake only in the vessel wall and plaques. It is corrected by blood pool FDG level, and therefore, normalized for background activity.<sup>20,53</sup> TBR is also robust in different scanning settings of emission time and filter, while SUV has significant difference in each of these settings.<sup>32</sup> TBRmean and TBRmax both are reproducible<sup>17</sup> and have been used in many studies showing association with inflammation,<sup>46</sup> cardiovascular events,<sup>37</sup> and CVD risk factors.<sup>5</sup> FDG uptake, when measured as TBR, showed a significant correlation with macrophage level of the plaque<sup>1,7,25</sup> which is more than SUV correlation with the same factors.<sup>7</sup> The superiority of target-to-blood ratio over vessel uptake alone had been shown previously in other studies.<sup>47,63</sup> Some investigators have suggested that TBRmean may be better for evaluating total vessel wall inflammation, while TBRmax should be used for assessing atherosclerotic plaques.<sup>17</sup>

It is not clear which one of the introduced indices better reflect the actual FDG level taken up by the vessel walls and atherosclerosis lesions, and also which index is more related to inflammatory active parts of the vessel wall.<sup>64</sup> There is a requirement to perform a study which measures in vivo FDG uptake using various indices (i.e., SUVmean, SUVmax, blood pool-corrected SUV, partial volume-corrected SUV, TBRmean, and TBRmax) and then ex vivo indices (well counting PET and micro PET) to figure out which in vivo index is compatible with ex vivo measurement of the FDG level in the plaques.

As mentioned before, although there are some reports showing the association between clinical records and outcomes with FDG uptake in the vessel walls, we need a study to compare the value of each one of FDG measurement indices in differentiating patients with different CVD risk factors and also predicting the clinical outcome.

### **Index Vessel Selection, Most Diseased Segments, and Active Segments**

**Index vessel selection.** Evaluation of FDG uptake activity in the index vessel has been introduced by investigators to show the effects of new therapeutics

on vessel walls.<sup>14,59,65</sup> In this method, FDG levels should be measured in some vessels (i.e., ascending aorta and carotid) and the vessel with the highest baseline activity would be selected as the index vessel. This vessel is later used to evaluate the effect of therapies on atherosclerosis and inflammation. Using this method, investigators could compare the vessels which are more diseased and may better show the effect of interventions.<sup>14,18,59</sup> Superiority of the methods using vessel with the highest baseline FDG uptake activity (index vessel) over other methods evaluating similar anatomical vessels (carotid vs carotid or aorta vs aorta) for evaluation and comparison between groups is not clear. In the studies showing that the same vessels have significantly different FDG uptake between groups, index vessel may or may not be able to show this difference.<sup>18,65</sup> Additionally, investigators must compare a combination of carotid and aorta as index vessel between patients, while these vessels are not the same in progression of atherosclerosis, remodeling of vessels, response to therapies,<sup>66</sup> and biological and pathological conditions.<sup>45</sup> Because there may be a combination of vessels (i.e., carotid and ascending aorta) defined as index vessel, a single cut-off points may not be good for detecting atherosclerosis and inflammation in the vessel walls.<sup>4,5,45,56,67</sup> Fayad ZA et al reported that ascending aorta was more probable to be designated as the index vessel<sup>65</sup> which reduces the participation of carotid arteries in the final results. This will largely confound the final results if the disease or treatment effect is more detectable by PET in the carotid arteries but the aorta is selected as the index vessel.<sup>45,65</sup>

**Segment-based analysis.** It is reasonable to use predefined targets when we are evaluating the effects of an intervention on vessel wall and atherosclerotic inflammation.<sup>13,59</sup> Investigators have tried to detect the diseased segments of a vessel because these areas are mostly targeted by interventions and better reveal the effects of the treatments on the vessel wall plaques. These sections could be the most diseased<sup>14,65</sup> or active segments<sup>13,59</sup> detected in either the index vessel<sup>14,42,59,65</sup> or all vessels.<sup>13</sup> These target segments were recorded by measuring the distance from landmarks (carotid bifurcation for the carotid arteries and top of the aortic arch for the ascending aorta) to repeat the measurements and compare their findings before and after therapy.<sup>13,14,59,65</sup>

**Most diseased segment.** The slice with the highest FDG uptake activity and the surrounding slices below and above would be defined as the most diseased segment (Figure 2).<sup>14,65</sup> Because the most diseased segment is supposed to be the portion of the vessel with the highest atherosclerosis and inflammatory disease, it may be more sensitive to show the effect of treatments on the vessel wall plaques.<sup>13,14,68</sup> The FDG uptake of the most

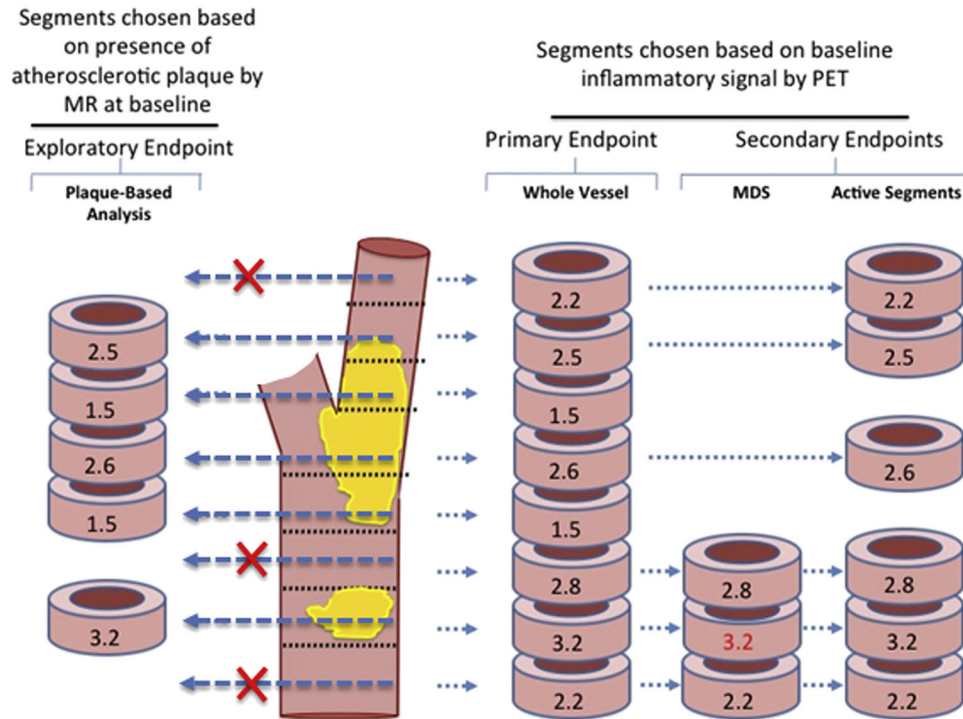


**Figure 2.** Most diseased segment: the slice with the highest TBR and the surrounding slices immediately above and below were selected as the most diseased segments. These areas were then evaluated before and after therapy to determine the effect of intervention on vessel wall metabolic activity. Active Segments: segments with TBR  $\geq 1.6$  were considered as active segments and would be reevaluated after therapy to see the effects of drugs on atherosclerosis Image reused from Tawakol et al<sup>42</sup>.

diseased segment should be measured before and after interventions and compared between these two time points to assess the effect of the therapies.

**Active segments.** By defining a cut-off point for FDG uptake of vessel wall, some transverse slices with FDG level greater than this threshold will be considered active segments where the atherosclerosis and inflammation are located (Figure 2). These segments may better show the effect of interventions than whole vessel evaluations which assess both diseased and healthy segments.<sup>38,59</sup> After defining the active segments, there are potentially two methods that can be applied to evaluate the effects of therapies on the vessels. In the first method, the semi-quantitative index of FDG level (i.e., TBR or SUV), which is evaluated at the baseline, should be compared to the post-therapeutic levels.<sup>59</sup> In the other method, the number of active segments should be compared between pre- and post-therapy FDG-PET scans.<sup>13,38,59</sup> A problem with active segment evaluation is the lack of a universally accepted cut-off point for detecting atherosclerosis. The reported threshold has varied as differently as TBRmax  $\geq 1.6$ ,<sup>59</sup> TBRmax  $\geq 1.7$ ,<sup>5</sup> SUVmax  $> 2.0$ ,<sup>31</sup> SUVmax  $\geq 2.7$ ,<sup>69</sup> SUVmax  $> 2.5$ <sup>70</sup> as well as other numbers.<sup>29</sup>

Although segment-based analyses that include most diseased segment and active segment methods seem promising for further interventional studies, an important potential bias with these methods is known as “transient phenomenon.” This term has been used to describe cases where arterial lesions with increased FDG uptake activity on baseline scans do not show similar activity levels in subsequent scans. In extreme cases, it has been shown that even some of the primarily active slices may not show increased FDG uptake activity in later PET images regardless of the drugs administered to patients during the elapsed time.<sup>56</sup> This could be related to the cell biology of atherosclerosis resulting in repeated episodes of plaque inflammation, rupture, and remodeling. Moreover, it may be due to infections and change in medications after first scans which may influence the degree of plaque inflammation and glycolysis.<sup>62</sup> On the other hand, this phenomenon may be due to technical aspects of imaging and small changes in bed positions in repeated scans. Transient phenomenon should be considered when specific segments are evaluated in the later scans. These segments may or may not show increased FDG uptake activity in the next scan.

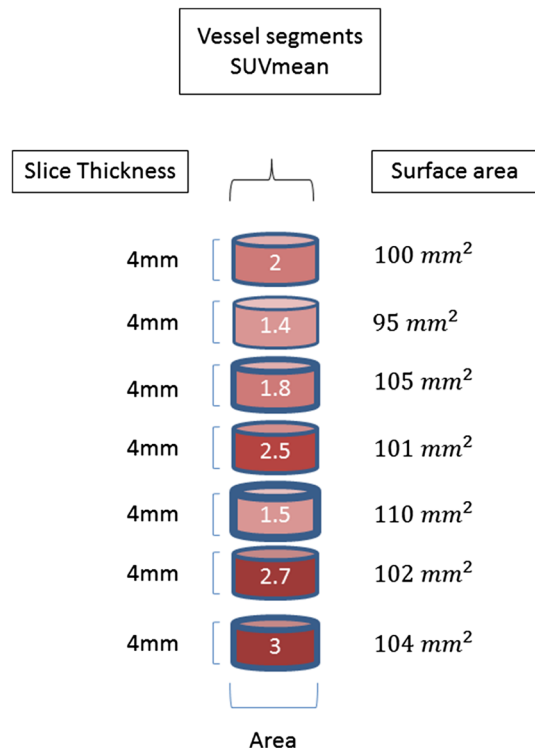


**Figure 3.** Global inflammatory burden: sum of metabolic volumetric product of consecutive segments. In this method, regions of interest are placed around the carotid wall in every slice (7 slices each is 4 mm in length) and metabolic volumetric product of each slice will be calculated as  $SUV_{mean} \times \text{Slice area} \times \text{Slice length}$ . The metabolic volumetric product of the second lowermost slice is  $2.7 \times 102 \text{ mm}^2 \times 4 \text{ mm} = 1101.6 \text{ mm}^3$ . Metabolic volumetric product of a vessel segment is named global inflammatory burden and is the sum of the consecutive slices' metabolic volumetric product. Global inflammatory burden is the sum of metabolic volumetric product of multiple parts of that vessel (i.e., for aorta, the global inflammatory burden of ascending, arch, descending, and abdominal aorta should be summed to reach global inflammatory burden of the aorta). Regions without metabolic activity minimally contribute to the metabolic volumetric product, so this is valid as an index of active plaques<sup>16</sup>.

### Methods Using Vessel Wall Structure in Addition to FDG Uptake Activity

FDG-PET/CT-based measurements such as SUV and TBR only give information about metabolic activity of the vessel wall and atherosclerosis but not about the structure and extension of the plaques. Vessel wall diameter, transverse area, and length of the diseased vessel are structural characteristics that have been associated with further vascular events.<sup>71,72</sup> Change in the vascular transverse area is associated with vascular wall remodeling in the setting of atherosclerosis and is

commonly seen as vascular enlargement.<sup>66,73,74</sup> This change is associated with unstable plaques and higher incidence of cardiovascular events.<sup>75</sup> Vessel transverse area is sensitive to anti-atherosclerosis treatments<sup>65,66</sup> and is associated with increased FDG uptake activity.<sup>65,76,77</sup> FDG-PET/CT can provide information about the metabolic state, morphology, extension, and structure of the vessel wall and atherosclerotic lesions.<sup>2</sup> There are some methods introduced in the literature that evaluate both metabolic and structural aspects of vessel walls. These methods are trying to measure atherosclerosis burden,<sup>44</sup> global inflammatory burden,<sup>16</sup> and global metabolic activity.<sup>78</sup>

**Global inflammatory burden.** Vessel FDG uptake (SUV) is multiplied by vessel trans-axial area ( $\text{mm}^2$ ) and slice length (mm) to calculate metabolic volumetric product of each transverse slice.<sup>16,43</sup> Then, the metabolic volumetric products of consecutive slices are summed to determine the metabolic volumetric product of each vessel segment (i.e., common carotid) (Figure 3).<sup>16,43</sup> Finally, the metabolic volumetric products of consecutive segments of a vessel (i.e., ascending, arch, descending, and abdominal parts of aorta) are summed to calculate the global inflammatory burden of the whole vessel (aorta).<sup>16,43</sup>

**Atherosclerosis burden and global metabolic activity.** Vessel wall thickness (measured in images of contrast-enhanced CT or magnetic resonance imaging (MRI)) is multiplied by slice length to calculate the volume of vessel wall at each transverse slice. Then, in each slice, the vessel wall volume is multiplied by SUV<sub>mean</sub> to determine the atherosclerotic burden.<sup>44</sup> Since calcification is not metabolically active and does not accumulate FDG, wall calcification is then subtracted from the vessel wall volume to calculate the net volume of the wall. Finally, the net volume is multiplied by SUV<sub>mean</sub> to calculate global metabolic activity.<sup>78</sup>

In the methods using both structural and metabolic aspects of a vessel to evaluate inflammation and atherosclerosis, transverse slices with minimal metabolic activity will have less contribution to final measurement and the results would be valid for metabolically active parts of the vessels.<sup>43</sup> These methods may require contrast enhancement to have more accurate estimation of vessel diameter and wall thickness. These measurement methods are dependent to length and width of the vessels which is not the same across patients. It may be helpful to normalize the final score by the length and width of measured vessel segment or to limit the number of slices to a constant number then normalize the measurement for the vessel wall thickness or diameter.

## Coverage Extension and Slice Skipping

In coverage extension, the target vessel length would be extended from a single vessel (i.e., common carotid) to the segments proximal and distal to it (ascending aorta and internal carotid, respectively).<sup>45</sup> Extension of the coverage was suggested because it was shown that diseases associated with atherosclerosis such as stroke occur when there is atherosclerotic involvement of sufficient length in the carotid.<sup>45,71</sup> Extending the plaque inflammatory activity measurements to a longer segment including ascending aorta, common carotid, and internal carotid has shown a reasonable correlation and agreement with FDG uptake measurements of common carotid alone.<sup>45</sup> But it is noticeable that TBR scores increase when internal carotid and/or ascending aorta are added to common carotid (common carotid alone vs extended coverage to internal carotid and/or ascending aorta).<sup>45</sup> It may be due to different rate of atherosclerosis development and risk factors associated with atherosclerosis and FDG uptake activity in each one of these vessels.<sup>45,66,79</sup>

In addition to the metabolic activity shown by FDG uptake indices, coverage extension may be a method for including the length of atherosclerotic lesion as an important factor for future CVD events. However, because vessels may have different baseline and disease-associated FDG uptake activities, considering vessels as a single target may result in some biases.

**Slice skipping.** When assessment should be done for a long length of vessels or coverage extension is applied, workload of FDG uptake measurement increases and much more time is needed to perform the study. To decrease the work burden and the time needed to make measurements, investigators have devised numerous methods including one side carotid measurements instead of two sides,<sup>40,80</sup> measuring a fraction of vessels<sup>76</sup> and slice skipping.<sup>45</sup> In the latter method, which occurs after coverage extension, some transverse slices are skipped regularly (1 of 2 or 2 of 3 consecutive slices should be skipped) to reduce the workload and, therefore, resulting in less time spent on making the measurements.<sup>45</sup> A drawback of these workload lightening methods is the probability of missing some highly active plaques which would play major role in future cardiovascular events.

## PARTIAL VOLUME EFFECT CORRECTION

The thickness of vessel walls as well as the size of atherosclerotic plaques is typically smaller than 3 mm,<sup>81,82</sup> which is less than the spatial resolution of the available clinical PET machines (4 mm). As shown by phantom studies, partial volume correction may

significantly affect FDG uptake measurements in the vessel walls.<sup>83</sup> There have been some clinical studies that have tried to introduce an effective method for reducing partial volume effect and spillover activity using MRI<sup>84</sup> and contrast enhance CT scan.<sup>85</sup> However, these studies have reported controversial results. Therefore, a future study that compares the various partial volume correction methods with each other and with the findings of phantom studies is necessary to determine the most accurate and reproducible method.

## WHICH VESSEL SHOULD BE MEASURED?

Investigators may seek local atherosclerotic activity in the carotids and vertebral arteries for cerebrovascular disease<sup>24</sup> as well as peripheral vessels for peripheral vascular diseases.<sup>86,87</sup> Alternatively, because atherosclerosis is a systemic disease that can involve multiple vessels at the same time,<sup>88</sup> investigators may plan to evaluate one or few parts of the vascular system to find the general atherosclerotic activity in a subject. Commonly evaluated vessels include whole aorta,<sup>4,13</sup> aorta segments,<sup>37,38</sup> carotids,<sup>5</sup> and other vessels.<sup>89,90</sup>

Measuring FDG uptake in the coronary arteries has some problems (please see section *Evaluation of coronary arteries atherosclerosis using FDG-PET/CT* below). Therefore, there is a question about the most appropriate large vessel that best reflects the coronary arteries atherosclerosis. Although there are some reports about the association of atherosclerosis prevalence, distribution, and morphology of aorta and carotids with coronaries,<sup>91-95</sup> there should be a FDG-PET/CT-based study that compares these large vessels with coronary artery histopathology findings, clinical symptoms, and short- and long-term cardiovascular outcomes to determine the most appropriate vessel.

## EVALUATION OF CORONARY ARTERIES ATHEROSCLEROSIS USING FDG-PET/CT

Many acute coronary syndrome events happen due to rupture of atherosclerosis plaques with less than 50% stenosis. As a result, there is an increasing interest toward evaluating molecular activity of the plaques. There are some reports on the capability of FDG-PET/CT to visualize coronary artery atherosclerosis in diabetic patients<sup>46</sup> and atherosclerosis plaques before<sup>96,97</sup> and after stenting.<sup>57</sup>

Despite the potential applicability of this technique, there are some concerns with its applications for visualizing the coronary arteries. These include the high avidity of the cardiomyocytes for FDG which affects differentiation and measurement of coronary arteries,<sup>98,99</sup> motion artifacts due to cardiac and respiratory



activities which impedes accurate vascular co-registration and photon detection,<sup>57,99,100</sup> and limited spatial resolution of available PET/CT machines (3-5 mm).<sup>100,101</sup> Some solutions have been introduced for these issues. For example, myocardial FDG uptake can be controlled by specific diet restrictions (low carbohydrate and high fat),<sup>98,102</sup> and cardiac motion effects can be reduced by administering beta blockers prior to PET imaging or applying electrocardiography and respiratory gating<sup>103,104</sup> and motion tracking with 4D CT or PET.<sup>99,105</sup> Although these approaches seem promising, it is important to note that restricted diet<sup>102</sup> and gated imaging<sup>57</sup> have not always been helpful. Finally, resources should be utilized for developing specialized PET/CT machines with increased spatial resolution for evaluating small arteries.<sup>46</sup>

### ACTION PLAN

FDG-PET/CT is a promising imaging strategy to evaluate atherosclerosis. In this review, we showed the diversity of methodologies used by research groups. Non-unified patient preparation and image acquisition protocols and quantification indices may result in inconsistent findings. Therefore, developing standardized protocols seems necessary.

Some studies should be implemented to evaluate the effects of diet instruction and pre-scan blood glucose level on the atherosclerotic uptake of FDG and its association with clinical and histopathology findings to reach an optimized and a standardized protocol.

Although there are some reports, the efficacy of delayed time point FDG-PET/CT imaging to accurately diagnose disease patterns still needs to be confirmed by studies that compare early vs. delayed time point imaging.

Another step is to figure out which in vivo measurement index best reflects the true value of FDG uptake in the vessel wall, and whether this true value correlates with vessel wall histopathological characteristics. Investigators should also determine the measurement index that is most correlated with the clinical presentation of the patients and predictive of future cardiovascular events.

Despite some improvements, there are still many obstacles in evaluating coronary atherosclerosis with FDG-PET/CT and studies should be focused on optimizing the methods for suppressing cardiac FDG uptake, reducing cardiac motion effects, and improving spatial resolution of the imaging tools. At this time, we need to find the most appropriate large vessel in the body that best correlates with coronary atherosclerotic developments, CVD symptoms, and further cardiovascular events. Alternately, the development of other radiotracers that

are not taken up by cardiac muscle cells could be a potential avenue for visualizing the coronary arteries accurately. However, in all scenarios, the use of partial volume-corrected global assessments to measure the general uptake of the coronary vasculature systems is necessary for accurate quantification of disease activity.

### References

1. Tawakol A, Migrino RQ, Bashian GG, Bedri S, Vermylen D, Cury RC, et al. In vivo 18F-fluorodeoxyglucose positron emission tomography imaging provides a noninvasive measure of carotid plaque inflammation in patients. *J Am Coll Cardiol* 2006;48:1818-24.
2. Chen W, Bural GG, Torigian DA, Rader DJ, Alavi A. Emerging role of FDG-PET/CT in assessing atherosclerosis in large arteries. *Eur J Nucl Med Mol Imaging* 2009;36:144-51.
3. Yun M, Yeh D, Araujo LI, Jang S, Newberg A, Alavi A. F-18 FDG uptake in the large arteries: A new observation. *Clin Nucl Med* 2001;26:314-9.
4. Bural GG, Torigian DA, Chamroonrat W, Houseni M, Chen W, Basu S, et al. FDG-PET is an effective imaging modality to detect and quantify age-related atherosclerosis in large arteries. *Eur J Nucl Med Mol Imaging* 2008;35:562-9.
5. Noh TS, Moon SH, Cho YS, Hong SP, Lee EJ, Choi JY, et al. Relation of carotid artery 18F-FDG uptake to C-reactive protein and Framingham risk score in a large cohort of asymptomatic adults. *J Nucl Med* 2013;54:2070-6.
6. Hag AM, Pedersen SF, Christoffersen C, Binderup T, Jensen MM, Jorgensen JT, et al. (18) F-FDG PET imaging of murine atherosclerosis: Association with gene expression of key molecular markers. *PLoS One* 2012;7:e50908.
7. Zhao QM, Feng TT, Zhao X, Xu ZM, Liu Y, Li DP, et al. Imaging of atherosclerotic aorta of rabbit model by detection of plaque inflammation with fluorine-18 fluorodeoxyglucose positron emission tomography/computed tomography. *Chin Med J (Engl)* 2011;124:911-7.
8. Zhao QM, Zhao X, Feng TT, Zhang MD, Zhuang XC, Zhao XC, et al. Monitoring of atherosclerosis evolution by detection of inflammatory states of aortae in a rabbit model using 18F-FDG-PET/CT. *Q J Nucl Med Mol Imaging* 2014;58:440-50.
9. Worthley SG, Zhang ZY, Machac J, Helft G, Tang C, Liew GY, et al. In vivo non-invasive serial monitoring of FDG-PET progression and regression in a rabbit model of atherosclerosis. *Int J Cardiovasc Imaging* 2009;25:251-7.
10. Wallis deVries BM, van Dam GM, Tio RA, Hillebrands JL, Slart RH, Zeebregts CJ. Current imaging modalities to visualize vulnerability within the atherosclerotic carotid plaque. *J Vasc Surg* 2008;48:1620-29.
11. Ogawa M, Magata Y, Kato T, Hatano K, Ishino S, Mukai T, et al. Application of 18F-FDG PET for monitoring the therapeutic effect of antiinflammatory drugs on stabilization of vulnerable atherosclerotic plaques. *J Nucl Med* 2006;47:1845-50.
12. Rudd JH, Myers KS, Bansilal S, Machac J, Rafique A, Farkouh M, et al. (18)Fluorodeoxyglucose positron emission tomography imaging of atherosclerotic plaque inflammation is highly reproducible: Implications for atherosclerosis therapy trials. *J Am Coll Cardiol* 2007;50:892-6.
13. Tahara N, Kai H, Ishibashi M, Nakaura H, Kaida H, Baba K, et al. Simvastatin attenuates plaque inflammation: Evaluation by fluorodeoxyglucose positron emission tomography. *J Am Coll Cardiol* 2006;48:1825-31.

14. Tawakol A, Fayad ZA, Mogg R, Alon A, Klimas MT, Dansky H, et al. Intensification of statin therapy results in a rapid reduction in atherosclerotic inflammation: Results of a multicenter fluorodeoxyglucose-positron emission tomography/computed tomography feasibility study. *J Am Coll Cardiol* 2013;62:909-17.
15. Kobayashi Y, Ishii K, Oda K, Nariai T, Tanaka Y, Ishiwata K, et al. Aortic wall inflammation due to Takayasu arteritis imaged with 18F-FDG PET coregistered with enhanced CT. *J Nucl Med* 2005;46:917-22.
16. Rose S, Sheth NH, Baker JF, Ogdie A, Raper A, Saboury B, et al. A comparison of vascular inflammation in psoriasis, rheumatoid arthritis, and healthy subjects by FDG-PET/CT: A pilot study. *Am J Cardiovasc Dis* 2013;3:273-8.
17. Rudd JH, Myers KS, Bansilal S, Machac J, Pinto CA, Tong C, et al. Atherosclerosis inflammation imaging with 18F-FDG PET: Carotid, iliac, and femoral uptake reproducibility, quantification methods, and recommendations. *J Nucl Med* 2008;49:871-8.
18. Bissonnette R, Tardif JC, Harel F, Pressacco J, Bolduc C, Guertin MC. Effects of the tumor necrosis factor-alpha antagonist adalimumab on arterial inflammation assessed by positron emission tomography in patients with psoriasis: Results of a randomized controlled trial. *Circ Cardiovasc Imaging* 2013;6:83-90.
19. Blomberg BA, Thomassen A, Takx RA, Hildebrandt MG, Simonsen JA, Buch-Olsen KM, et al. Delayed (1)(8)F-fluorodeoxyglucose PET/CT imaging improves quantitation of atherosclerotic plaque inflammation: Results from the CAMONA study. *J Nucl Cardiol* 2014;21:588-97.
20. Bucnerius J, Mani V, Moncrieff C, Machac J, Fuster V, Farkouh ME, et al. Optimizing 18F-FDG PET/CT imaging of vessel wall inflammation: The impact of 18F-FDG circulation time, injected dose, uptake parameters, and fasting blood glucose levels. *Eur J Nucl Med Mol Imaging* 2014;41:369-83.
21. Kim EJ, Kim S, Kang DO, Seo HS. Metabolic activity of the spleen and bone marrow in patients with acute myocardial infarction evaluated by 18F-fluorodeoxyglucose positron emission tomographic imaging. *Circ Cardiovasc Imaging* 2014;7:454-60.
22. Wasselius JA, Larsson SA, Jacobsson H. FDG-accumulating atherosclerotic plaques identified with 18F-FDG-PET/CT in 141 patients. *Mol Imaging Biol* 2009;11:455-9.
23. Duijvenvoorden R, Mani V, Woodward M, Kallend D, Suchankova G, Fuster V, et al. Relationship of serum inflammatory biomarkers with plaque inflammation assessed by FDG PET/CT: The dal-PLAQUE study. *JACC Cardiovasc Imaging* 2013;6:1087-94.
24. Davies JR, Rudd JH, Fryer TD, Graves MJ, Clark JC, Kirkpatrick PJ, et al. Identification of culprit lesions after transient ischemic attack by combined 18F fluorodeoxyglucose positron-emission tomography and high-resolution magnetic resonance imaging. *Stroke* 2005;36:2642-7.
25. Figueroa AL, Subramanian SS, Cury RC, Truong QA, Gardecki JA, Tearney GJ, et al. Distribution of inflammation within carotid atherosclerotic plaques with high-risk morphological features: A comparison between positron emission tomography activity, plaque morphology, and histopathology. *Circ Cardiovasc Imaging* 2012;5:69-77.
26. Fifer KM, Qadir S, Subramanian S, Vijayakumar J, Figueroa AL, Truong QA, et al. Positron emission tomography measurement of periodontal 18F-fluorodeoxyglucose uptake is associated with histologically determined carotid plaque inflammation. *J Am Coll Cardiol* 2011;57:971-6.
27. Font MA, Fernandez A, Carvajal A, Gamez C, Badimon L, Slevin M, et al. Imaging of early inflammation in low-to-moderate carotid stenosis by 18-FDG-PET. *Front Biosci* 2009;14:3352-60.
28. Yarasheski KE, Laciny E, Overton ET, Reeds DN, Harrod M, Baldwin S, et al. 18FDG PET-CT imaging detects arterial inflammation and early atherosclerosis in HIV-infected adults with cardiovascular disease risk factors. *J Inflamm (Lond)* 2012;9:26.
29. Menezes LJ, Kotze CW, Hutton BF, Endozo R, Dickson JC, Cullum I, et al. Vascular inflammation imaging with 18F-FDG PET/CT: When to image? *J Nucl Med* 2009;50:854-7.
30. Rudd JH, Machac J, Fayad ZA. Simvastatin and plaque inflammation. *J Am Coll Cardiol* 2007;49:1991; author reply-2.
31. Wu YW, Kao HL, Chen MF, Lee BC, Tseng WY, Jeng JS, et al. Characterization of plaques using 18F-FDG PET/CT in patients with carotid atherosclerosis and correlation with matrix metalloproteinase-1. *J Nucl Med* 2007;48:227-33.
32. Graebe M, Borgwardt L, Hojgaard L, Sillesen H, Kjaer A. When to image carotid plaque inflammation with FDG PET/CT. *Nucl Med Commun* 2010;31:773-9.
33. Rudd JH, Warburton EA, Fryer TD, Jones HA, Clark JC, Antoun N, et al. Imaging atherosclerotic plaque inflammation with [18F]-fluorodeoxyglucose positron emission tomography. *Circulation* 2002;105:2708-11.
34. Rudd JH, Myers KS, Bansilal S, Machac J, Woodward M, Fuster V, et al. Relationships among regional arterial inflammation, calcification, risk factors, and biomarkers: A prospective fluorodeoxyglucose positron-emission tomography/computed tomography imaging study. *Circ Cardiovasc Imaging* 2009;2:107-15.
35. Yun M, Jang S, Cucchiara A, Newberg AB, Alavi A. 18F FDG uptake in the large arteries: A correlation study with the atherogenic risk factors. *Semin Nucl Med* 2002;32:70-6.
36. Ryu Y, Yoshida K, Suzuki Y, Nakadate M, Umehara I, Tomita M, et al. Long-term changes of aortic 18F-FDG uptake and calcification in health-screening subjects. *Ann Nucl Med* 2013;27:239-46.
37. Figueroa AL, Abdelbaky A, Truong QA, Corsini E, MacNabb MH, Lavender ZR, et al. Measurement of arterial activity on routine FDG PET/CT images improves prediction of risk of future CV events. *JACC Cardiovasc Imaging* 2013;6:1250-9.
38. Paulmier B, Duet M, Khayat R, Pierquet-Ghazzar N, Laissy JP, Maunoury C, et al. Arterial wall uptake of fluorodeoxyglucose on PET imaging in stable cancer disease patients indicates higher risk for cardiovascular events. *J Nucl Cardiol* 2008;15:209-17.
39. Fayad ZA, Mani V, Woodward M, Kallend D, Bansilal S, Pozza J, et al. Rationale and design of dal-PLAQUE: A study assessing efficacy and safety of dalcetrapib on progression or regression of atherosclerosis using magnetic resonance imaging and 18F-fluorodeoxyglucose positron emission tomography/computed tomography. *Am Heart J* 2011;162:e2.
40. Kim TN, Kim S, Yang SJ, Yoo HJ, Seo JA, Kim SG, et al. Vascular inflammation in patients with impaired glucose tolerance and type 2 diabetes: Analysis with 18F-fluorodeoxyglucose positron emission tomography. *Circ Cardiovasc Imaging* 2010;3:142-8.
41. Kwee RM, Teule GJ, van Oostenbrugge RJ, Mess WH, Prins MH, van der Geest RJ, et al. Multimodality imaging of carotid artery plaques: 18F-fluoro-2-deoxyglucose positron emission tomography, computed tomography, and magnetic resonance imaging. *Stroke* 2009;40:3718-24.
42. Tawakol A, Singh P, Rudd JH, Soffer J, Cai G, Vucic E, et al. Effect of treatment for 12 weeks with rilapladib, a lipoprotein-associated phospholipase A2 inhibitor, on arterial inflammation as assessed with 18F-fluorodeoxyglucose-positron emission tomography imaging. *J Am Coll Cardiol* 2014;63:86-8.
43. Mehta NN, Torigian DA, Gelfand JM, Saboury B, Alavi A. Quantification of atherosclerotic plaque activity and vascular inflammation using [18-F] fluorodeoxyglucose positron emission

- tomography/computed tomography (FDG-PET/CT). *J Vis Exp* 2012;63:e3777.
44. Bural GG, Torigian DA, Chamroonrat W, Alkhaldeh K, Houseni M, El-Haddad G, et al. Quantitative assessment of the atherosclerotic burden of the aorta by combined FDG-PET and CT image analysis: A new concept. *Nucl Med Biol* 2006;33:1037-43.
  45. Noh TS, Yoo J, Kim SW, Lee EJ, Choi JY, Kim BT, et al. Effects of coverage extent and slice skipping on mean and maximum arterial 18F-FDG uptake ratios in patients with carotid plaque. *Ann Nucl Med* 2012;26:715-22.
  46. Nitta Y, Tahara N, Tahara A, Honda A, Kodama N, Mizoguchi M, et al. Pioglitazone decreases coronary artery inflammation in impaired glucose tolerance and diabetes mellitus: Evaluation by FDG-PET/CT imaging. *JACC Cardiovasc Imaging* 2013;6:1172-82.
  47. Ogawa M, Ishino S, Mukai T, Asano D, Teramoto N, Watabe H, et al. (18)F-FDG accumulation in atherosclerotic plaques: Immunohistochemical and PET imaging study. *J Nucl Med* 2004;45:1245-50.
  48. Ishino S, Ogawa M, Mori I, Nishimura S, Ikeda S, Sugita T, et al. 18F-FDG PET and intravascular ultrasonography (IVUS) images compared with histology of atherosclerotic plaques: 18F-FDG accumulates in foamy macrophages. *Eur J Nucl Med Mol Imaging* 2014;41:624-33.
  49. Thie JA. Understanding the standardized uptake value, its methods, and implications for usage. *J Nucl Med* 2004;45:1431-4.
  50. Vucic E, Calcagno C, Dickson SD, Rudd JH, Hayashi K, Bucerius J, et al. Regression of inflammation in atherosclerosis by the LXR agonist R211945: A noninvasive assessment and comparison with atorvastatin. *JACC Cardiovasc Imaging* 2012;5:819-28.
  51. Bucerius J, Mani V, Moncrieff C, Rudd JH, Machac J, Fuster V, et al. Impact of noninsulin-dependent type 2 diabetes on carotid wall 18F-fluorodeoxyglucose positron emission tomography uptake. *J Am Coll Cardiol* 2012;59:2080-8.
  52. Millon A, Dickson SD, Klink A, Izquierdo-Garcia D, Bini J, Lancelot E, et al. Monitoring plaque inflammation in atherosclerotic rabbits with an iron oxide (P904) and (18)F-FDG using a combined PET/MR scanner. *Atherosclerosis* 2013;228:339-45.
  53. Bai B, Bading J, Conti PS. Tumor quantification in clinical positron emission tomography. *Theranostics* 2013;3:787-801.
  54. Calcagno C, Ramachandran S, Izquierdo-Garcia D, Mani V, Millon A, Rosenbaum D, et al. The complementary roles of dynamic contrast-enhanced MRI and 18F-fluorodeoxyglucose PET/CT for imaging of carotid atherosclerosis. *Eur J Nucl Med Mol Imaging* 2013;40:1884-93.
  55. Jaipersad AS, Shantsila A, Lip GY, Shantsila E. Expression of monocyte subsets and angiogenic markers in relation to carotid plaque neovascularization in patients with pre-existing coronary artery disease and carotid stenosis. *Ann Med* 2014;46:530-8.
  56. Menezes LJ, Kayani I, Ben-Haim S, Hutton B, Ell PJ, Groves AM. What is the natural history of 18F-FDG uptake in arterial atheroma on PET/CT? Implications for imaging the vulnerable plaque. *Atherosclerosis* 2010;211:136-40.
  57. Rogers IS, Nasir K, Figueroa AL, Cury RC, Hoffmann U, Vermylen DA, et al. Feasibility of FDG imaging of the coronary arteries: Comparison between acute coronary syndrome and stable angina. *JACC Cardiovasc Imaging* 2010;3:388-97.
  58. Wu YW, Kao HL, Huang CL, Chen MF, Lin LY, Wang YC, et al. The effects of 3-month atorvastatin therapy on arterial inflammation, calcification, abdominal adipose tissue and circulating biomarkers. *Eur J Nucl Med Mol Imaging* 2012;39:399-407.
  59. Elkhawad M, Rudd JH, Sarov-Blat L, Cai G, Wells R, Davies LC, et al. Effects of p38 mitogen-activated protein kinase inhibition on vascular and systemic inflammation in patients with atherosclerosis. *JACC Cardiovasc Imaging* 2012;5:911-22.
  60. Bucerius J, Mani V, Wong S, Moncrieff C, Izquierdo-Garcia D, Machac J, et al. Arterial and fat tissue inflammation are highly correlated: A prospective 18F-FDG PET/CT study. *Eur J Nucl Med Mol Imaging* 2014;41:934-45.
  61. Subramanian S, Emami H, Vucic E, Singh P, Vijayakumar J, Fifer KM, et al. High-dose atorvastatin reduces periodontal inflammation: A novel pleiotropic effect of statins. *J Am Coll Cardiol* 2013;62:2382-91.
  62. Emami H, Vijayakumar J, Subramanian S, Vucic E, Singh P, MacNabb MH, et al. Arterial 18F-FDG uptake in rheumatoid arthritis correlates with synovial activity. *JACC Cardiovasc Imaging* 2014;7:959-60.
  63. Zhang Z, Machac J, Helft G, Worthley SG, Tang C, Zaman AG, et al. Non-invasive imaging of atherosclerotic plaque macrophage in a rabbit model with F-18 FDG PET: A histopathological correlation. *BMC Nucl Med* 2006;6:3.
  64. Sadeghi MM. 18F-FDG PET and vascular inflammation: Time to refine the paradigm? *J Nucl Cardiol* 2014. doi:10.1007/s12350-014-9917-1.
  65. Fayad ZA, Mani V, Woodward M, Kallend D, Abt M, Burgess T, et al. Safety and efficacy of dalcetrapib on atherosclerotic disease using novel non-invasive multimodality imaging (dal-PLAQUE): A randomised clinical trial. *Lancet* 2011;378:1547-59.
  66. Hayashi K, Mani V, Nemade A, Aguiar S, Postley JE, Fuster V, et al. Variations in atherosclerosis and remodeling patterns in aorta and carotids. *J Cardiovasc Magn Reson* 2010;12:10.
  67. Rominger A, Saam T, Wolpers S, Cyran CC, Schmidt M, Forster S, et al. 18F-FDG PET/CT identifies patients at risk for future vascular events in an otherwise asymptomatic cohort with neoplastic disease. *J Nucl Med* 2009;50:1611-20.
  68. Lee JM, Wiesmann F, Shirodaria C, Leeson P, Petersen SE, Francis JM, et al. Early changes in arterial structure and function following statin initiation: Quantification by magnetic resonance imaging. *Atherosclerosis* 2008;197:951-8.
  69. Arauz A, Hoyos L, Zenteno M, Mendoza R, Alexanderson E. Carotid plaque inflammation detected by 18F-fluorodeoxyglucose-positron emission tomography. Pilot study. *Clin Neurol Neurosurg* 2007;109:409-12.
  70. Kuehl H, Eggebrecht H, Boes T, Antoch G, Rosenbaum S, Ladd S, et al. Detection of inflammation in patients with acute aortic syndrome: Comparison of FDG-PET/CT imaging and serological markers of inflammation. *Heart* 2008;94:1472-7.
  71. Arora S, Chien JD, Cheng SC, Chun KA, Wintermark M. Optimal carotid artery coverage for carotid plaque CT-imaging in predicting ischemic stroke. *J Neuroradiol* 2010;37:98-103.
  72. Tresoldi S, Di Leo G, Zoffoli E, Munari A, Primolevo A, Cornalba G, et al. Association of aortic wall thickness on contrast-enhanced chest CT with major cerebro-cardiac events. *Acta Radiol* 2013;55:1040-9.
  73. Crouse JR 3rd. Thematic review series: Patient-oriented research. Imaging atherosclerosis: State of the art. *J Lipid Res* 2006;47:1677-99.
  74. Glagov S, Weisenberg E, Zarins CK, Stankunavicius R, Kolettis GJ. Compensatory enlargement of human atherosclerotic coronary arteries. *N Engl J Med*. 1987;316:1371-5.
  75. Schoenhagen P, Ziada KM, Kapadia SR, Crowe TD, Nissen SE, Tuzcu EM. Extent and direction of arterial remodeling in stable versus unstable coronary syndromes: An intravascular ultrasound study. *Circulation* 2000;101:598-603.

76. Tahara N, Kai H, Yamagishi S, Mizoguchi M, Nakaura H, Ishibashi M, et al. Vascular inflammation evaluated by [18F]-fluorodeoxyglucose positron emission tomography is associated with the metabolic syndrome. *J Am Coll Cardiol* 2007;49:1533-9.
77. Silvera SS, Aidi HE, Rudd JH, Mani V, Yang L, Farkouh M, et al. Multimodality imaging of atherosclerotic plaque activity and composition using FDG-PET/CT and MRI in carotid and femoral arteries. *Atherosclerosis* 2009;207:139-43.
78. Bural GG, Torigan DA, Botvinick E, Houseni M, Basu S, Chen W, et al. A pilot study of changes in (18)F-FDG uptake, calcification and global metabolic activity of the aorta with aging. *Hell J Nucl Med* 2009;12:123-8.
79. Strobl FF, Rominger A, Wolpers S, Rist C, Bamberg F, Thierfelder KM, et al. Impact of cardiovascular risk factors on vessel wall inflammation and calcified plaque burden differs across vascular beds: A PET-CT study. *Int J Cardiovasc Imaging* 2013;29:1899-908.
80. Okane K, Ibaraki M, Toyoshima H, Sugawara S, Takahashi K, Miura S, et al. 18F-FDG accumulation in atherosclerosis: Use of CT and MR co-registration of thoracic and carotid arteries. *Eur J Nucl Med Mol Imaging* 2006;33:589-94.
81. Mensel B, Quadrat A, Schneider T, Kuhn JP, Dorr M, Volzke H, et al. MRI-based determination of reference values of thoracic aortic wall thickness in a general population. *Eur Radiol* 2014;24:2038-44.
82. Shakeri A, Hafez Quran F, Javadrashid R, Abdekarimi MH, Ghojzadeh M, Abolghassemi Fakhree MB. Correlation between Aortic wall thickness and coronary artery disease by 64 slice multidetector computed tomography. *J Cardiovasc Thorac Res* 2013;5:91-5.
83. Burg S, Dupas A, Stute S, Dieudonne A, Huet P, Le Guludec D, et al. Partial volume effect estimation and correction in the aortic vascular wall in PET imaging. *Phys Med Biol* 2013;58:7527-42.
84. Izquierdo-Garcia D, Davies JR, Graves MJ, Rudd JH, Gillard JH, Weissberg PL, et al. Comparison of methods for magnetic resonance-guided [18-F]fluorodeoxyglucose positron emission tomography in human carotid arteries: Reproducibility, partial volume correction, and correlation between methods. *Stroke* 2009;40:86-93.
85. Houshmand S, Gholami S, Salavati A, Bashyam A, Ramachandran A, Werner T, et al. Accurate quantification of aortic wall inflammation using FDG-PET/CT: A method for partial volume effect correction based on contrast enhanced computed tomography. In: Annual congress of the european association of nuclear medicine, Gothenburg; 2014.
86. Nawaz A, Saboury B, Basu S, Zhuang H, Moghadam-Kia S, Werner T, et al. Relation between popliteal-tibial artery atherosclerosis and global glycolytic metabolism in the affected diabetic foot: A pilot study using quantitative FDG-PET. *J Am Podiatr Med Assoc* 2012;102:240-6.
87. Basu S, Zhuang H, Alavi A. Imaging of lower extremity artery atherosclerosis in diabetic foot: FDG-PET imaging and histopathological correlates. *Clin Nucl Med* 2007;32:567-8.
88. Strong JP, Malcom GT, McMahan CA, Tracy RE, Newman WP 3rd, Herderick EE, et al. Prevalence and extent of atherosclerosis in adolescents and young adults: Implications for prevention from the Pathobiological Determinants of Atherosclerosis in Youth Study. *JAMA* 1999;281:727-35.
89. Morbelli S, Ghigliotti G, Spinella G, Marini C, Bossert I, Cimmino MA, et al. Systemic vascular inflammation in abdominal aortic aneurysm patients: A contrast-enhanced PET/CT study. *Q J Nucl Med Mol Imaging* 2014;58:299-309.
90. Orellana MR, Bentourkia M, Sarrhini O, Fulop T, Paquet N, Lavallee E, et al. Assessment of inflammation in large arteries with 18F-FDG-PET in elderly. *Comput Med Imaging Graph* 2013;37:459-65.
91. Roos CJ, Witkowska AJ, de Graaf MA, Veltman CE, Delgado V, de Grooth GJ, et al. Association of atherosclerosis in the descending thoracic aorta with coronary artery disease on multi detector row computed tomography coronary angiography in patients with suspected coronary artery disease. *Int J Cardiovasc Imaging* 2013;29:1829-37.
92. Thej MJ, Kalyani R, Kiran J. Atherosclerosis in coronary artery and aorta in a semi-urban population by applying modified American Heart Association classification of atherosclerosis: An autopsy study. *J Cardiovasc Dis Res* 2012;3:265-71.
93. Agmon Y, Khandheria BK, Meissner I, Schwartz GL, Petterson TM, O'Fallon WM, et al. Relation of coronary artery disease and cerebrovascular disease with atherosclerosis of the thoracic aorta in the general population. *Am J Cardiol* 2002;89:262-7.
94. McGill HC Jr, McMahan CA, Herderick EE, Tracy RE, Malcom GT, Zieske AW, et al. Effects of coronary heart disease risk factors on atherosclerosis of selected regions of the aorta and right coronary artery. PDAY Research Group. Pathobiological Determinants of Atherosclerosis in Youth. *Arterioscler Thromb Vasc Biol* 2000;20:836-45.
95. Rohani M, Jogestrund T, Ekberg M, van der Linden J, Kallner G, Jussila R, et al. Interrelation between the extent of atherosclerosis in the thoracic aorta, carotid intima-media thickness and the extent of coronary artery disease. *Atherosclerosis* 2005;179:311-6.
96. Alexanderson E, Slomka P, Cheng V, Meave A, Saldana Y, Garcia-Rojas L, et al. Fusion of positron emission tomography and coronary computed tomographic angiography identifies fluorine 18 fluorodeoxyglucose uptake in the left main coronary artery soft plaque. *J Nucl Cardiol* 2008;15:841-3.
97. Saam T, Rominger A, Wolpers S, Nikolaou K, Rist C, Greif M, et al. Association of inflammation of the left anterior descending coronary artery with cardiovascular risk factors, plaque burden and pericardial fat volume: A PET/CT study. *Eur J Nucl Med Mol Imaging* 2010;37:1203-12.
98. Wykrzykowska J, Lehman S, Williams G, Parker JA, Palmer MR, Varkey S, et al. Imaging of inflamed and vulnerable plaque in coronary arteries with 18F-FDG PET/CT in patients with suppression of myocardial uptake using a low-carbohydrate, high-fat preparation. *J Nucl Med* 2009;50:563-8.
99. Tarkin JM, Joshi FR, Rudd JH. PET imaging of inflammation in atherosclerosis. *Nat Rev Cardiol* 2014;11:443-57.
100. Hucker WJ, Jaffer FA. F-FDG PET imaging of atherosclerosis—A new approach to detect inflamed, high-risk coronary plaques? *Curr Cardiovasc Imaging Rep* 2011;4:1-3.
101. Leuschner F, Nahrendorf M. Molecular imaging of coronary atherosclerosis and myocardial infarction: Considerations for the bench and perspectives for the clinic. *Circ Res* 2011;108:593-606.
102. Kumar P, Patel CD, Singla S, Malhotra A. Effect of duration of fasting and diet on the myocardial uptake of F-18-2-fluoro-2-deoxyglucose (F-18 FDG) at rest. *Indian J Nucl Med* 2014;29:140-5.
103. Buther F, Dawood M, Stegger L, Wubbeling F, Schafers M, Schober O, et al. List mode-driven cardiac and respiratory gating in PET. *J Nucl Med* 2009;50:674-81.
104. Chen W, Dilsizian V. (18)F-fluorodeoxyglucose PET imaging of coronary atherosclerosis and plaque inflammation. *Curr Cardiol Rep* 2010;12:179-84.
105. Fayad HJ, Lamare F, Le Rest CC, Bettinardi V, Visvikis D. Generation of 4-dimensional CT images based on 4-dimensional PET-derived motion fields. *J Nucl Med* 2013;54:631-8.